INTERNATIONAL SOCIETY FOR SOIL MECHANICS AND GEOTECHNICAL ENGINEERING



This paper was downloaded from the Online Library of the International Society for Soil Mechanics and Geotechnical Engineering (ISSMGE). The library is available here:

https://www.issmge.org/publications/online-library

This is an open-access database that archives thousands of papers published under the Auspices of the ISSMGE and maintained by the Innovation and Development Committee of ISSMGE.

The paper was published in the proceedings of the 20th International Conference on Soil Mechanics and Geotechnical Engineering and was edited by Mizanur Rahman and Mark Jaksa. The conference was held from May 1st to May 5th 2022 in Sydney, Australia.

Investigation of mud flow from boreholes during horizontal directional drilling

Étude de la circulation de la boue de forage lors du forage directionnel horizontal.

Ian Moore & Haitao Lan

GeoEngineering Centre at Queen's - RMC, Queen's University, Canada, ian.moore@queensu.ca

ABSTRACT: Horizontal directional drilling is used extensively for installation of pipelines under roads, railways, rivers, and other obstructions. Transport of drilling mud to the ground surface needs to be controlled to avoid damage to other infrastructure and the environment. Extensive physical modeling involved testing in the laboratory using 38 mm diameter boreholes to investigate the geomechanical processes, with 9 different experiments used to obtain pressure histories for mud escaping from boreholes at a range of depths, and 10 used to examine the influence of pumping rates and stratigraphy. Measurements of surface deformation during the mud flow process were also made. Post-test exhumations detailed the mud flow paths and mechanisms. The tests show that mud pressures rise quickly, then pass a peak and descend slowly as mud moves up to the ground surface. Little surface movement develops until well after the peak mud pressure (ground movements develop largely because of the added volume of mud entering the sand). The study includes measurements of earth pressures in the vicinity of the borehole. A new design equation has been developed, and the impact of stratified coarse grained soils is also investigated.

RÉSUMÉ: Le forage directionnel horizontal est grandement utilisé lors de l'installation des pipelines sous les routes, les voies ferrées, les cours d'eau et autres obstacles. Le transport de la boue de forage à la surface doit être contrôlé pour éviter tout dommage aux infrastructures existantes et à l'environnement. Des modélisations physiques approfondies ont été menées en laboratoire en utilisant des trous de forage de 38 mm de diamètre afin d'étudier les processus géomécaniques, incluant 9 essais visant à obtenir l'historique des pressions de boue s'échappant des trous de forage à diverses profondeurs, ainsi que 10 autres expériences menées pour examiner l'influence du taux de pompage et de la stratigraphie. Les déformations à la surface ont été mesurées durant le processus de circulation de la boue de forage. Les exhumations après essai ont fourni des détails sur la circulation de la boue et les mécanismes impliqués. L'analyse des résultats montre que les pressions de boue de forage augmentent rapidement pour atteindre un sommet, puis redescend lentement lorsque la boue de forage approche de la surface. Il y a peu de mouvement à la surface du sol, jusqu'à ce que le maximum des pressions soit largement dépassé (les mouvements à la surface du sol se développent alors en raison du volume additionnel de boue de dans le sable). L'étude inclut des mesures de la pression des terres près du trou de forage. Une nouvelle équation est développée pour la conception; l'impact des sols grossiers stratifiés est aussi étudié.

KEYWORDS: trenchless construction, directional drilling, pipeline installation, mud flow, failure.

1 INTRODUCTION

Horizontal Directional Drilling (HDD) can be used when pipeline installation encounters obstacles, like rivers and lakes. Although directional drilling has been applied for decades, there are still concerns related to this method. One issue is horizontal borehole stability during pilot hole drilling (followed by reaming and then pipeline pull-back into the borehole). To prevent borehole collapse when drilling in sand, mud is pumped into the borehole. However, if mud pressure is too high, tensile or shear failure could occur around the borehole (Lan and Moore, 2017), leading to inadvertent mud return (mud transport to the surface).

Therefore, it is important to estimate the maximum allowable mud pressure P_{max} and work to stay under this limit during the drilling process. The so-called Delft Equation (Luger and Hergarden, 1988) and modified by Keulen (2001) is often used to estimate maximum mud pressure. However, this has been questioned by Xia and Moore (2006), Elwood et al. (2007), and Lan and Moore (2020) because the pressure calculated by the equation is not safe and many inadvertent returns have been reported when this method is employed (e.g. Neher and Wallin, 2016). Problems with the Delft Equation include: (1) it is based on cavity expansion theory which is inappropriate because the initial geostatic stresses in the field are anisotropic rather than isotropic; (2) two key quantity choices assumed to coincide with the mud pressure limit lack supporting evidence: the value of R_{max} (the outer radius of the plastic region around the borehole) is assumed to be two-thirds of the distance to the ground surface for cohesionless soil, or pressure is calculated to ensure tensile hoop strain just reaches 5% (Dutch standard NEN 3650-1+C1).

A series of medium scale experiments were conducted by Lan (2018) to quantify P_{max} for sand. It is the first known effort to investigate how P_{max} is influenced by the ratio of burial depth (the distance from ground surface to borehole springline) to borehole diameter D (H/D), pump rates, and the behaviour of multi-layer systems (where dense sand containing the borehole is covered by different thicknesses of dense sandy gravel or loose sand). This paper illustrates the physical modeling with an example experiment, outlines the finite element modeling of the experiments, and summarizes the new design equation developed based on those experimental and numerical investigations.

2 EXPERIMENTS

2.1 Test apparatus and procedures

Tests were conducted in a pit 2 m wide, 2 m long and 2 m deep. The north, east and south walls were made of concrete while the west side was a temporary timber retaining wall (Fig.1(a)). All were sufficiently stiff to prevent lateral movements during testing. A uniform sand ("Hydro-Sand") was employed as defined in Table 1 (see Lan and Moore, 2020 for more details).

Three main steps were used in each test: backfilling, mud pumping, and exhumation:

(1) Backfilling. Sand was placed in 200 to 250 mm layers and compacted by a vibrating plate packer. Average Proctor density achieved was around 90%. Burial depth (H) was varied by using different numbers of layers, while the borehole diameter (D) was maintained constant. To investigate pump rate, H/D was kept at 18. For tests involving loose sand or dense sandy gravel, H/D

was kept almost constant but different thicknesses of loose sand (H_{loose}) or dense sandy gravel (H_G) , (compacted to average proctor density of 85%) were used so different H_{loose}/H or

Table 1. Properties of Hydro-Sand and sandy gravel.

| Type | Properties | Value |
|-----------------|--|-------|
| Hydro- Sand | 100% Proctor Density (kg/m^3) | 1745 |
| | K_0^{-1} | 0.51 |
| | Poisson Ratio | 0.3 |
| | Peak Friction Angle ² ϕ_p' (°) | 46 |
| | Critical Friction Angle ² ϕ'_c (°) | 35 |
| | Maximum Dilation Angle ² ψ_{max} (°) | 19 |
| Sandy gravel | 100% Proctor Density (kg/m^3) | 2282 |
| | Poisson Ratio ³ | 0.3 |
| | Secant Modulus of Elasticity ³ (MPa) at | 60 |
| | confining pressure of 50 kPa | |
| | Peak Friction Angle ³ (°) | 56 |
| | Dilation Angle ³ (°) | 20 |

- 1: Average value obtained using null gauges
- 2: From isotropic consolidated drained triaxial tests at $\sigma_3' = 100 kPa$
- 3: Scott et al. (1977)

 H_G/H could be achieved. The surface was leveled, and targets were placed on the North side of the pit (Fig. 1). Target movements were captured by cameras installed on the East, West and South side of the wall, with images analyzed using Particle Image Velocity (PIV) (White et al., 2003). The procedure of Lan (2018) to remove 'pseudo-displacements' was then employed.

- (2) Mud pumping. A 38 mm diameter (D), 1.5 m long borehole was cut by a Shelby tube, 0.4 m above the bottom of the pit. A packer was inserted into the initial 0.5 m and inflated so sand near the borehole was densified and mud would not flow back to the West side of the wall. Borehole effective length (L) was 1 m, providing L/D of around 26. Distance from the center of the borehole to the side boundaries was 1 m. When the test started, mud was pumped through the packer into the borehole and mud pressure in the borehole was monitored by a transducer. The test was stopped when mud appeared at the ground surface.
- (3) Exhumation. After mud appeared at the surface, the mud travelling path was carefully excavated from the surface to the borehole. Water contents near the borehole were measured.

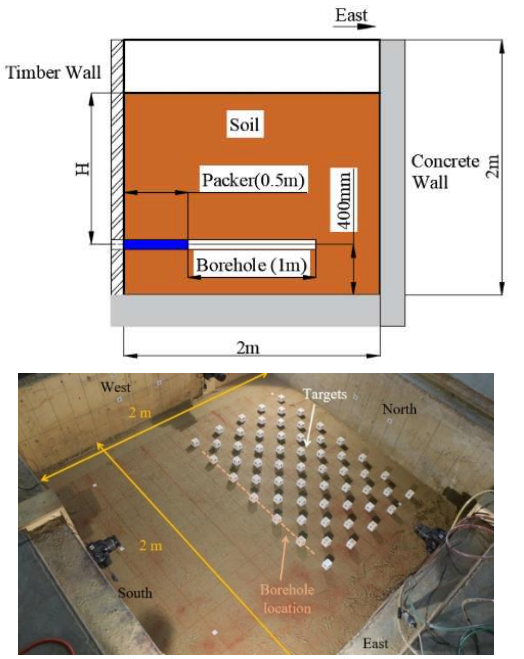


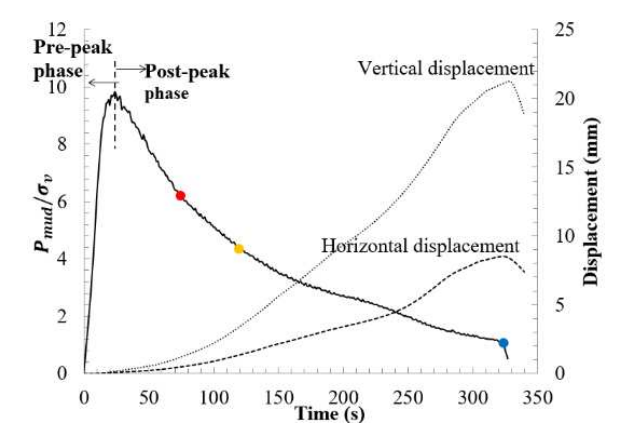
Figure 1. An example of test setup (a) configuration and (b) ground surface after backfilling (H/D=25).

2.2 Mud and earth pressure histories

Figure 2 presents the mud pressure and displacement histories from one particular test, where the mud pressure rises rapidly to a peak, then descends more slowly. Ground movements are negligible during the pre-peak phase, but become more significant during the post-peak phase as the volume of mud entering the sand rises. Surface uplift results in a primary crack at the surface running approximately parallel to the borehole, then secondary cracks. The mud appears beyond the cracked zone, having flowed up a shear plane above the borehole.

Although various stress analyses have been proposed (in particular, those based on cavity expansion theory), few measurements have been made of soil stresses near a borehole. Therefore, three earth pressure sensors of the kind developed by Talesnick (2013) (also called null gauges) were buried at distances of three times the borehole radius below the invert to measure axial, radial and hoop stresses.

Lan and Moore (2020) present the histories of mud pressure, hoop stress, axial and radial stresses obtained with the null gauges and compare them to stresses obtained from closed form solutions and numerical analyses, during the pre-peak phase, as illustrated in Figure 3. In the figure, the closed form solution is separated into an elastic response line and a plastic expansion line (Lan and Moore, 2017). The elastic response line is based on the Kirsch solution and the Mohr-Coulomb model was employed in the plastic analysis (Eq. 1). ABAQUS was used for the numerical analysis; further details are provided by Lan (2018).



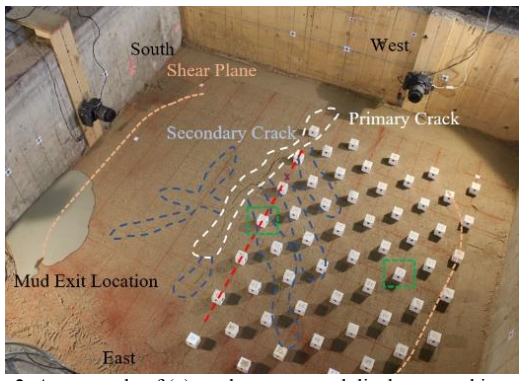


Figure 2. An example of (a) mud pressure and displacement histories (b) surface after testing (H/D=25); vertical displacement of green block at centre; horizontal displacement of green block at right.

When mud pressure increased initially, the hoop stresses decreased and the closed form solution and numerical models were close to the measured data. As mud pressure continued increasing, hoop stresses started to increase, and the closed form and numerical solutions followed the right tends (though noise in the measured data complicates the comparison). Experimental

data in the plastic region were between calculations for cohesion c=0 and 5 kPa. This may be due to mud infiltration around the borehole, which contributed to cohesion increase (so the plastic line moved downward). Details are given by Lan and Moore (2017).

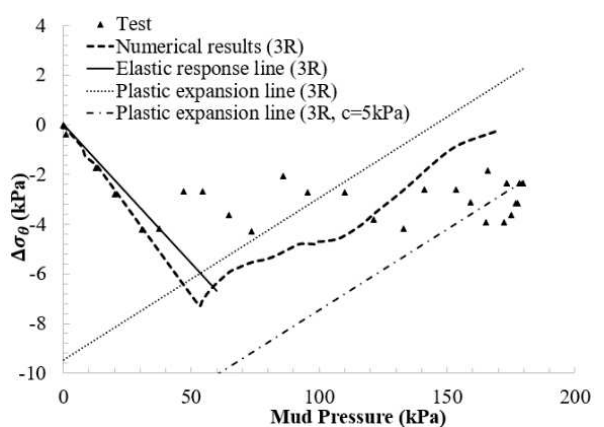


Figure 3. Comparison between stress measurement, closed form and numerical solutions (increment of hoop stress $\Delta\sigma_{\theta}$ versus mud pressure).

2.3 Mud travel paths

Figure 4 presents an example of a typical mud travel path composed of four sections, i.e. (1) the primary infiltration zone around the borehole; (2) several protrusions attached to the primary infiltration zone which develop at the onset of secondary cracks; (3) tubes connected to the primary infiltration zone or within the protrusions, with one ultimately connecting to the overlying shear plane; (4) the shear plane is like a 'sandwich' structure, where mud travels along the middle planar structure, two to five millimeters thick. These experiments represent the first investigation where mud travel paths were explicitly investigated, with that pathway seen to have geometry significantly different to those assumed in the analyses.

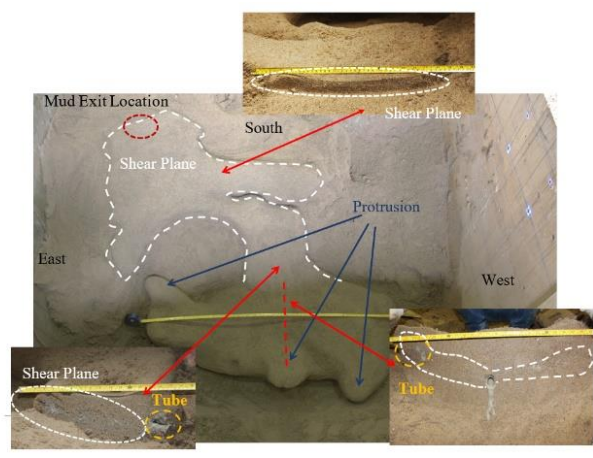


Figure 4 Example of mud travel path (H/D=25).

2.4 Effect of burial depths, pump rates and multi-layer systems

The peak mud pressures in these tests are given by Lan (2018) and Lan and Moore (2020). It was observed that: (1) the peak mud pressure increased steadily as burial depths increased; (2) peak mud pressure was found to be independent of the pump rates (where those were scaled to reflect typical field condition); (3) when multi-layered systems are involved, the pressure went

up with increase of H_{loose}/H_{\perp} and decreased with increase in H_C/H .

3 DESIGN EQUATION

Although the numerical analysis was supported by the experimental data, the dimensions of the experiments do not represent those that occur in the field. Therefore, the side and bottom boundaries of the models were expanded and a parametric study was conducted (as detailed by Lan (2018)). Five friction angles were considered (30°, 35°, 40°, 45° and 50°, six values of H/D were examined (5, 10, 15, 20, 35 and 50) and four values of K_0 (0.4, 0.5, 0.7 and 1). The design equation for P_{max} was developed based on 120 simulations with curve fitting (Eq. 1).

$$\frac{P_{max}}{\sigma_v'} = 0.304 \left(\frac{H}{D}\right)^{\left[\left(\frac{1}{0.561\phi' - 9.887} + 0.078\right)\ln(K_0) + \left(0.4\ln(\phi') - 0.483\right)\right]} + 0.708$$
(1)

where, σ_v' is the effective vertical stress in kPa at the springline, the range of H/D is from 5 to 50; ϕ' is friction angle of the sand $(30^\circ \le \phi' \le 50^\circ)$, friction angle at critical state ϕ_c' for loose to medium sands, or the peak friction angle ϕ_p' for medium dense to dense sands; K_0 is the coefficient of lateral earth pressure at rest $(0.4 \le K_0 \le 1)$.

The results using this new design equation have been applied to data from several case studies and design criteria have been presented, i.e. the 'dangerous (unsafe) area' along the drilling path when the minimum mud pressure is higher than P_{max} where contractors should try to limit mud pressure so they do not induce inadvertent mud return during construction.

If the multi-layer systems were applied in the field, it is conservative to use this design equation when denser material is above while a reduction factor is needed when loose material is involved (see Lan (2018) for development of this reduction factor).

4 CONCLUSIONS

Horizontal borehole instability during HDD was investigated through a series of medium scale tests and numerical analyses. It is the first known effect to study how factors such as burial depth, pump rate and multi-layer systems influence this problem. The conclusions are:

- The maximum mud pressure supported within the borehole
 P_{max} increased with increasing burial depth, and was independent on the pump rates.
- Mud flow paths from the borehole to the ground surface were revealed. The paths included four zones.
- Based on the experimental evidence, numerical modeling was used to undertake a parametric study to develop a new design equation for P_{max} when drilling in sand.

5 ACKNOWLEDGEMENTS

The authors thank the Natural Sciences and Engineering Research Council of Canada (NSERC) and the Canada Foundation for Innovation (CFI) for funding this research. The authors are also grateful for assistance from Dr. Xuefeng Yan and Graeme Boyd during these experiments.

6 REFERENCES

- Elwood, D.E.Y., Moore, I.D., and Xia, H. 2007. Hydraulic fracture experiments in a frictional material and approximations for maximum allowable mud pressure. 60th Canadian Geotechnical Conference, Ottawa, Ontario, Canada, 1681-1688.
- Keulen, B. 2001. Maximum allowable pressures during directional drilling focused on sand. Delft Uni.of Tech. Delft.
- Lan, H. 2018. Experimental and numerical investigation of stability of horizontal boreholes during horizontal directional drilling. Ph.D. Thesis, Queen's University, Kingston, ON, Canada.
- Lan, H., and Moore, I.D. 2017. Numerical investigation of the circumferential stresses around boreholes during Horizontal Directional Drilling. *Int. J. Geomechanics*, 17(12), 04017114.
- Lan, H., and Moore, I.D. 2018. Practical criteria for assessment of horizontal borehole instability in saturated clay. *Tunnelling and Underground Space Technology*, 75(5), 21-35.
- Lan, H., and Moore, I.D. 2020. Experimental investigation examining influence of burial depth on stability of horizontal boreholes in sand. *J. Geotech. Geoenviron. Eng*, 145(12).
- Lan, H., Moore, I.D., and Dong, W. 2018. Measurement of ground heave due to horizontal borehole instability during Horizontal Directional Drilling experiments in sand. ASCE *Pipelines 2018: Planning and Design*, 373-383, Toronto, Canada.
- Luger, H.J., and Hergarden, H.J.A.M. 1988. Directional drilling in soft soil; influence of mud pressures. *Int. No-Dig Conf.* 1-7, Washington D.C. U.S.A..
- Neher, M. and Wallin, M. 2016. 36-inch HDD gas pipeline crossing of highway 880 in Fremont, CA. 2016 No-Dig show, WM-T1-02, Dallas, Texas, U.S.A..
- NEN 3650-1+C1. 2017. Requirements for pipeline systems Part 1: General requirements. Delft, Netherlands.
- Scott, J.D., Bauer, G.E., and Shields, D.H. (1977). Triaxial testing on granular aggregate. Ontario Joint Transportation and Communications Research Program, Ont. Project O-1.
- Talesnick, M. 2013. Measuring soil pressure within a soil mass. *Canadian Geotechnical J.*, 50(7), 716-722.
- White, D.J., Take, W.A., and Bolton, M.D. 2003. Soil deformation measurement using particle image velocimetry (PIV) and photogrammetry. *Géotechnique*, 53(7), 619-631.
- Xia, H., and Moore, I.D. 2006. Estimation of maximum mud pressure in purely cohesive material during directional drilling. *Geomechanics and GeoEngineering*, 1(1), 3-11.